Journal of Photochemistry and Photobiology A: Chemistry 218 (2011) 33–40

Contents lists available at ScienceDirect

Journal of Photochemistry and Photobiology A: Chemistry

journal homepage: www.elsevier.com/locate/jphotochem

An *ab initio* simulation of a dithienylethene/phenoxynaphthacenequinone photochromic hybrid

François Maurel[a], Aurélie Perrier[a], Denis Jacquemin[b,*]

[a] *Laboratoire Interfaces, Traitements, Organisation et Dynamique des Systèmes (ITODYS), UMR CNRS 7086, Université Paris Diderot, 15 rue Jean Antoine de Baïf, 75205 Paris Cedex 13, France*

[b] *Chimie et Interdisciplinarité: Synthèse, Analyse, Modélisation (CEISAM), UMR CNRS 6230, Université de Nantes, 2 rue de la Houssinière, BP 92208, 44322 Nantes Cedex 3, France*

ARTICLE INFO

Article history:
Received 5 October 2010
Received in revised form
17 November 2010
Accepted 25 November 2010
Available online 3 December 2010

Keywords:
Photochrome
Dithienylethene
Phenoxynaphthacenequinone
Time-Dependent Density Functional Theory

ABSTRACT

We simulate the properties of a photochromic blend synthesized by Myles, Wigglesworth and Branda [Adv. Mater. 15 (2003) 745] using *ab initio* tools. This hybrid multi-addressable molecular switch contains a dithienylethene moiety linked to a phenoxynaphthacenequinone group and exhibits four isomers with distinguishable excited-state features. In the first part of this work, we investigate the properties of model (isolated) dithienylethene and phenoxynaphthacenequinone photochromes, with a focus on the second family that was not fully characterized theoretically previously. In the second stage, the spectral properties of the blend are evaluated with the help of (Time-Dependent) Density Functional Theory.

1. Introduction

Photochromic entities may undergo a light-induced reversible transformation between two isomers presenting distinct absorption features [1,2]. Examples of photochromic families include azobenzenes (AB, *trans* ↔ *cis*), dithienylethenes (DT, *open* ↔ *closed*), phenoxynaphthacenequinones (PNQ, *trans* ↔ *ana*), naphthopyrans (NP, *spiro* ↔ *mero*) (see Fig. 1 for PNQ and DT). Obviously, if the properties of the two forms are significantly different, photochromes may act as main building blocks in on/off nano-devices. To increase the contrast between the two states, a convenient procedure is to plug a series of identical photochromes on a single conjugated core. In this way, the intensity of the extra visible absorption band appearing in the "on" state is strongly enhanced. A striking successful example of this strategy has been recently provided by Browne's and Feringa's groups [3]: a six-fold improvement was obtained with an extended multi-DA architecture. Nevertheless, this strategy suffers from two pitfalls [4,5]. On the one hand, in several cases the full photochromic activity is lost, so that the actual intensity enlargement is not proportional to the number of coupled photochromic units [6–9]. On the other hand, the position of the visible band of the absorption spectrum is almost insensitive to the number of switched molecules [9–11], so that the potential applications remain limited to "0/1" logical gates. To circumvent this latter drawback, combinations of (at least) two families of photochromes in a single molecule have been proposed, so that candidates for multifrequency optical memories can be designed. Only a few examples of such structures can be found in the literature and most undergo limitations: (1) the hybrid dithienylethene/hydroazulene synthesized by Mrozek et al. shows three out of four possible states [12,13], the last one being kinetically unstable; (2) the spirooxazine/chromene composite proposed by Favaro et al. allows the presence of more isomers but at the prize of a restrained photochromic reversibility [14,15]; (3) the spirooxazine/naphthopyran series proposed by Samat et al. also offers multiple isomers but the separation between the different visible bands is relatively small [16]; (4) the DT/PNQ mix designed by Branda's group (Fig. 2) [17], the focus of the present investigation, is, to our knowledge, the first structure displaying four possible photochromic forms with reversible transitions and well-distinguishable UV/vis signatures; (5) bi- and tri-photochromic composites formed of one DT and one (or two) side(s) naphthopyran(s), also display the desired features [18–21] and have been analyzed in a previous theoretical work [22]; (6) Pozzo's group recently created an hybrid molecule [23], with a indolinooxazolidine side group attached to a DT core, but due to the presence of side reactions, the fully conjugated form constitutes a deadlock in this system [23].

In the present investigation, we aim to use Time-Dependent Density Functional Theory (TD-DFT) [24,25] for simulating and analyzing the excited-states involved in all possible forms of the

* Corresponding author. Previous address: Unité de Chimie Physique Théorique et Structurale (UCPTS), Facultés Universitaires Notre-Dame de la Paix, rue de Bruxelles, 61, B-5000 Namur, Belgium. Tel.: +33 2 51 12 54 18; fax: +33 2 51 12 55 67.
E-mail address: Denis.Jacquemin@univ-nantes.fr (D. Jacquemin).

1010-6030/$ – see front matter © 2010 Elsevier B.V. All rights reserved.
doi:10.1016/j.jphotochem.2010.11.021

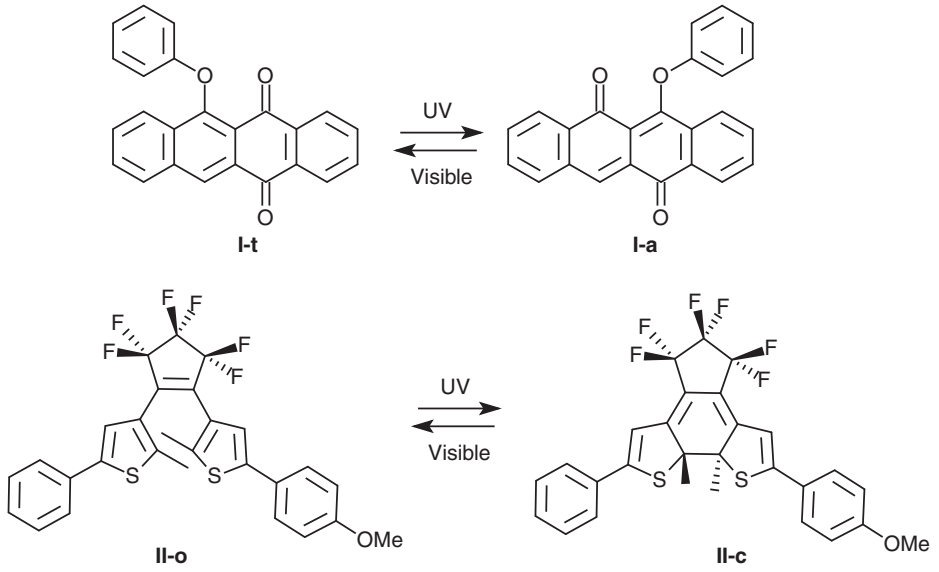

Fig. 1. Representation of the two model photochromic systems composing the hybrid switch: PNQ (top) and DT (bottom).

mixed DT/PNQ compound represented in Fig. 2. To this end, we have benchmarked specific DFT functionals and performed a short analysis of the PNQ isomerism with TD-DFT as, to the best of our knowledge, no similar theoretical investigation has been performed for this class of photochromes.

2. Computational details

Our simulations have followed a well-characterized protocol [26], that has recently been applied to another class of multiple-switch architecture [22]: (1) the ground-state structures have

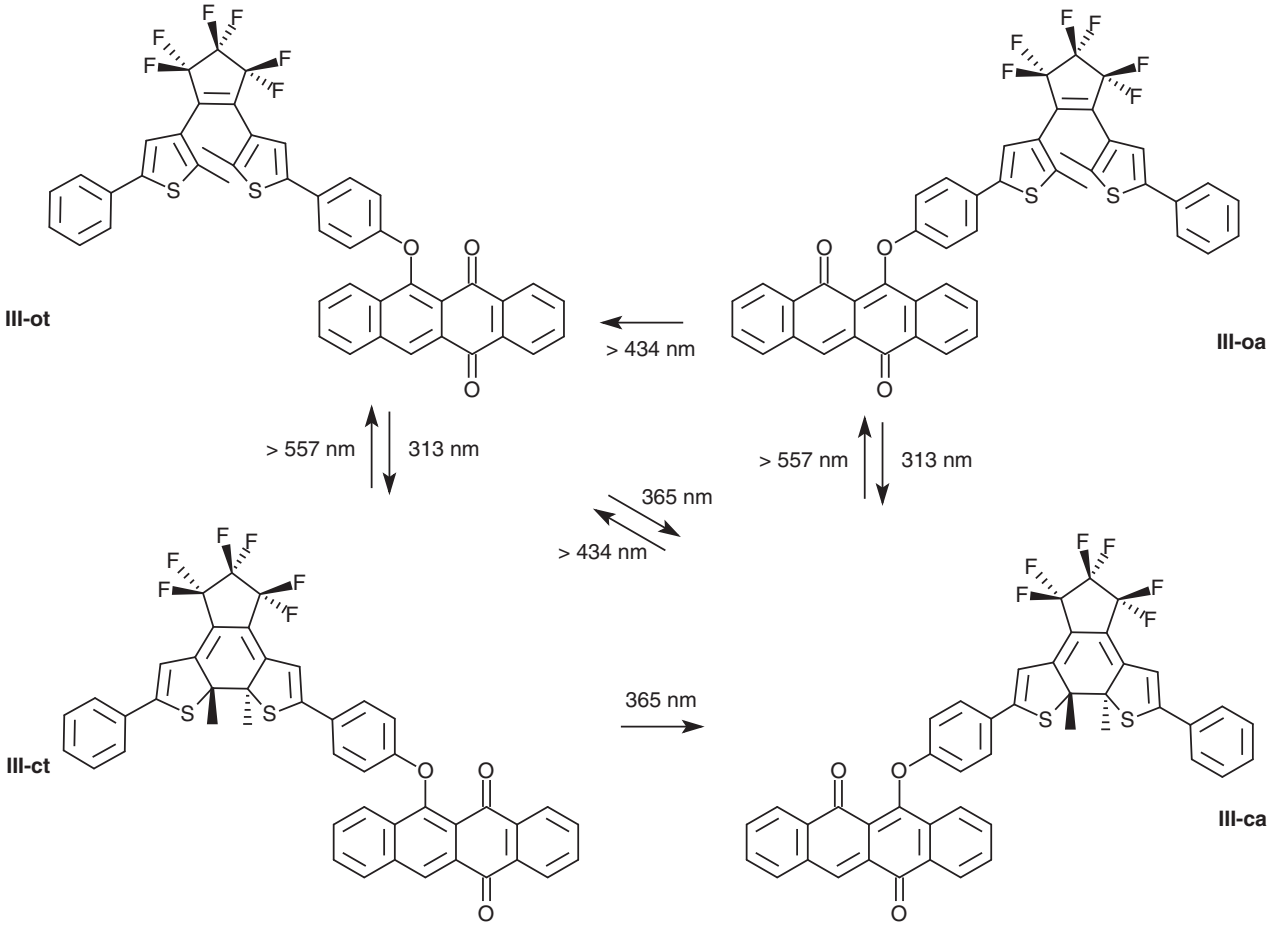

Fig. 2. Four possible isomers of the multi-addressable switch designed by Branda and coworkers [17]. The experimental operating wavelength and processes are also indicated.

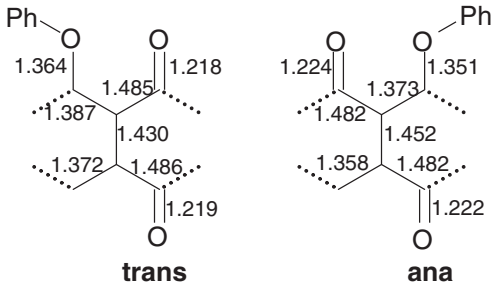

Fig. 3. Bond lengths in the central part of PNQ. All values are in Å and have been obtained at the PCM-PBE0/6-311G(d,p) level.

been minimized without symmetry constraints; (2) the vibrational frequencies have been computed so to ensure the absence of imaginary modes; (3) the vertical transition energies (and oscillator strengths) to the first ten lowest lying singlet excited-states have been computed. During the two first stages, the PBE0 [27,28]/6-311G(d,p) approach has been applied, as such approach provides converged geometrical parameters for most classes of dyes, including DT [29]. The third step, was performed with TD-DFT using a more extended basis set, namely 6-311+G(2d,p), that is suited for our purposes [29]. Three functionals have been tested: PBE0 [27,28], CAM-B3LYP [30] and ωB97XD [31]. This selection was made on the basis of previous benchmark calculations [32–35] that have demonstrated that these three functionals are amongst the most effective for medium-sized organic molecules. PBE0 is a global hybrid with a constant exact exchange percentage (25.0%), whereas CAM-B3LYP and ωB97XD are range-separated hybrids (RSH), relying on different parameters for both short-range (19.0% and 22.2%, respectively) and long-range exchanges (65.0% and 100.0%), as well as for the attenuation rate (0.33 $bohr^{-1}$ and 0.20 $bohr^{-1}$).

All calculations have been performed with the Gaussian09 program [36] using default thresholds and parameters, but for the SCF convergence criterion that has been systematically tightened (at least 10^{-8} a.u.) and the geometry optimization limits for which we selected the tight option. The bulk solvent (acetonitrile as in Ref. [17], except when noted) effects have been included at all stages (optimization, frequency calculations and TD-DFT simulations), by means of the Polarisable Continuum Model (PCM) [37].

3. Results and discussion

3.1. TD-DFT benchmarks

The characteristic wavelengths computed for the model DT and PNQ shown in Fig. 1 are compared to the experimental measurements of Ref. [17] in Table 1. DT have been widely investigated with DFT and TD-DFT previously [5,29,38–50] and only a brief analysis has been performed herein. From the data collated in Table 1, it is obvious that the tested functionals correctly reproduce the UV to visible shift of the λ_{max} noticed upon electrocyclization: the three methods provide satisfying estimates, CAM-B3LYP yielding the most accurate absorption wavelengths. Indeed, the CAM-B3LYP absolute errors are as small as 0.11 eV and 0.05 eV for the open and closed forms, respectively, whereas the deviations obtained with PBE0 (0.17 and 0.14 eV) or ωB97XD (0.15 and 0.08 eV) are slightly larger. These findings are consistent with previous benchmarks performed for both isolated [33,35,51] and coupled [5] DT.

Table 1
Comparisons between experimental (estimated from the UV/vis spectra of Ref. [17]) and theoretical λ_{max} (in nm) and oscillator strengths (between brackets) for the model PNQ and DT represented in Fig. 1. The simulated values have been obtained through the convolution (0.3 eV FWHM Gaussian) of the PCM(ACN)-TD-X/6-311+G(2d,p)//PCM(ACN)-PBE0/6-311G(d,p) transitions.

Method (X)	**I-t**	**I-a**	**II-o**	**II-c**
PBE0	389 (0.17)	492 (0.34)	302 (1.28)	636 (0.56)
CAM-B3LYP	348 (0.24)	451 (0.47)	283 (1.45)	577 (0.56)
ωB97XD	342 (0.26)	446 (0.48)	280 (1.49)	571 (0.54)
Experiment	390	478	290	592

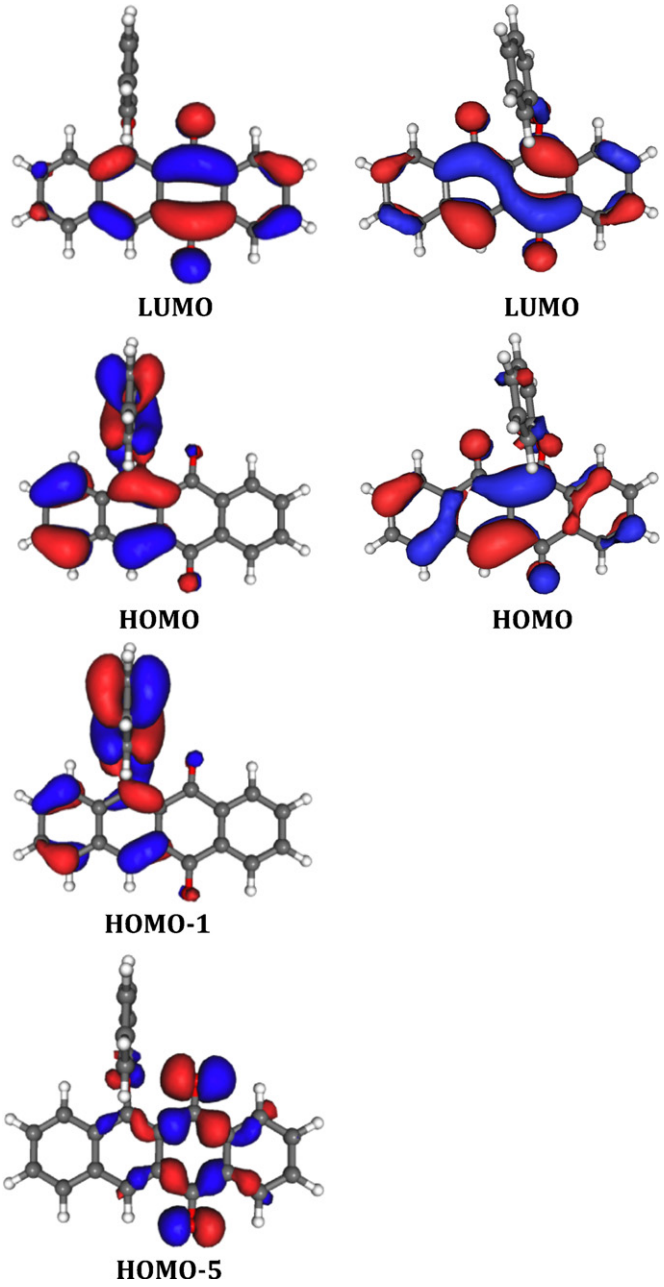

Fig. 4. Relevant CAM-B3LYP molecular orbitals for **I-t** (left) and **I-a** (right). A contour threshold of 0.03 a.u. has been used.

Experimentally, the *trans* form of PNQ presents a relatively weak absorption band close to 390 nm, that undergoes a significant bathochromic (~+90 nm) and hyperchromic shift (~×2) when converting to the *ana* isomer [17,52–54]. From the quantitative point of view, PBE0 performance is remarkable with errors below the 0.10 eV threshold for both *trans* and *ana* compounds, whereas the two RSH overestimate significantly the transition energies. This behavior parallels the results obtained for the parent anthraquinone dyes: global hybrids like PBE0 (and B3LYP) provide very accurate λ_{max} [51,55,56]. Nevertheless, as for DT, all three functionals qualitatively reproduce the spectral variations accom-

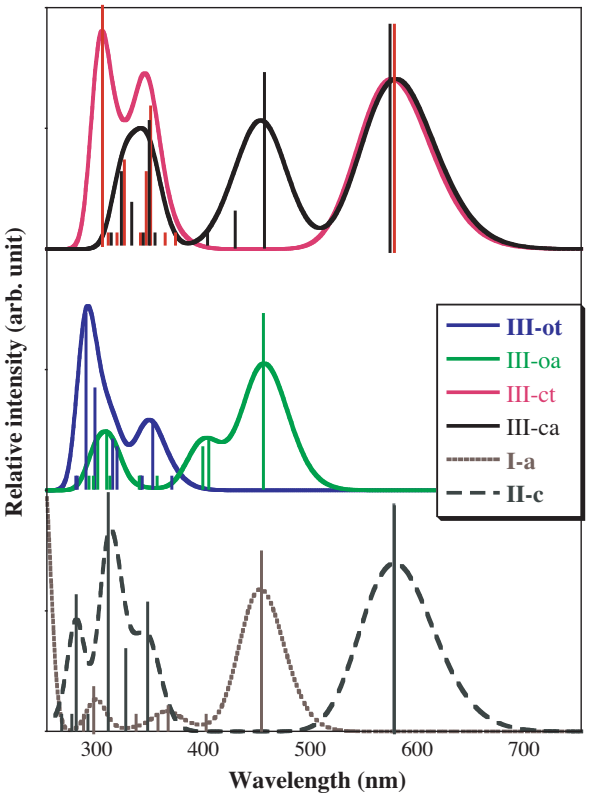

Fig. 5. Simulated UV/vis spectra of **III** (top) using CAM-B3LYP. The bottom of the graph shows the corresponding spectra for **I-a** and **II-c**. A broadening Gaussian of 0.3 eV has been used (see Table 2).

panying the photoisomerization of PNQ, so that there is little doubt that TD-DFT is an adequate tool for the mixed DT/PNQ switch.

As no single functional emerges as most accurate for both species, we have decided to perform the calculations on Branda's compound (Section 3.3) with both PBE0 and CAM-B3LYP. ωB97XD was discarded for providing errors systematically exceeding their CAM-B3LYP counterparts. For the records, PBE0 yields the smallest mean absolute deviation (MAD) [57], but it is known that RSH often deliver more consistent predictions [32–34,51,58–60], as well as "cleaner" molecular orbital analysis [61–63].

3.2. Phenoxynaphthacenequinone: trans and ana isomers

For PNQ, previous theoretical studies have mainly focussed on the impact of a connecting photochrome on the conducting properties of side electrodes [64,65], so that a longer discussion of the DFT and TD-DFT results is welcome. The *trans* isomer (**I-t**) is more stable than its *ana* counterpart (**I-a**) by 9.4 kcal mol^{-1} [Gibbs free energy with PCM-PBE0/6-311G(d,p)] or 10.0 kcal mol^{-1} [electronic energy with PCM-CAM-B3LYP/6-311+G(2d,p)]. These energetic differences can be compared to the typical values obtained for other classes of photochromes, e.g. DT (~10–15 kcal mol^{-1}) [5,66] and spirooxazines (~2–5 kcal mol^{-1}) [67–69]. The PCM-PBE0/6-311G(d,p) distances measured in the central part of both isomers can be found in Fig. 3. Upon photoisomerization, there is an obvious inversion of the single/double bond character for the four bonds vicinal to the transfered phenyl group: 1.364/1.387/1.485/1.218 Å for the *trans* form and 1.224/1.482/1.373/1.351 Å for the *ana* structure. This is perfectly consistent with chemical intuition (see Fig. 1) and is usual in photochromic reactions, e.g. DT also undergo a similar alteration. The other bonds are less affected by the photoisomerization. In fact, the bond length alternation (BLA) computed for the bonds represented in Fig. 3 are extremely similar for the less stable *ana* and more stable *trans* forms, indicating that the **I-t** → **I-a** reaction does not induce a very large modification of the electronic polarizability. The BLA is indeed directly related to electronic delocalization in π-conjugated systems [70]. Nevertheless, the dihedral angle between the central aromatic core and the side phenyl ring indicates a nearly perpendicular conformation for **I-t** (83°) but not for **I-a** (62°). Eventually, we note that, within the Mulliken approximation, all three oxygen atoms bear a charge of approximatively −0.5*e* in both isomers.

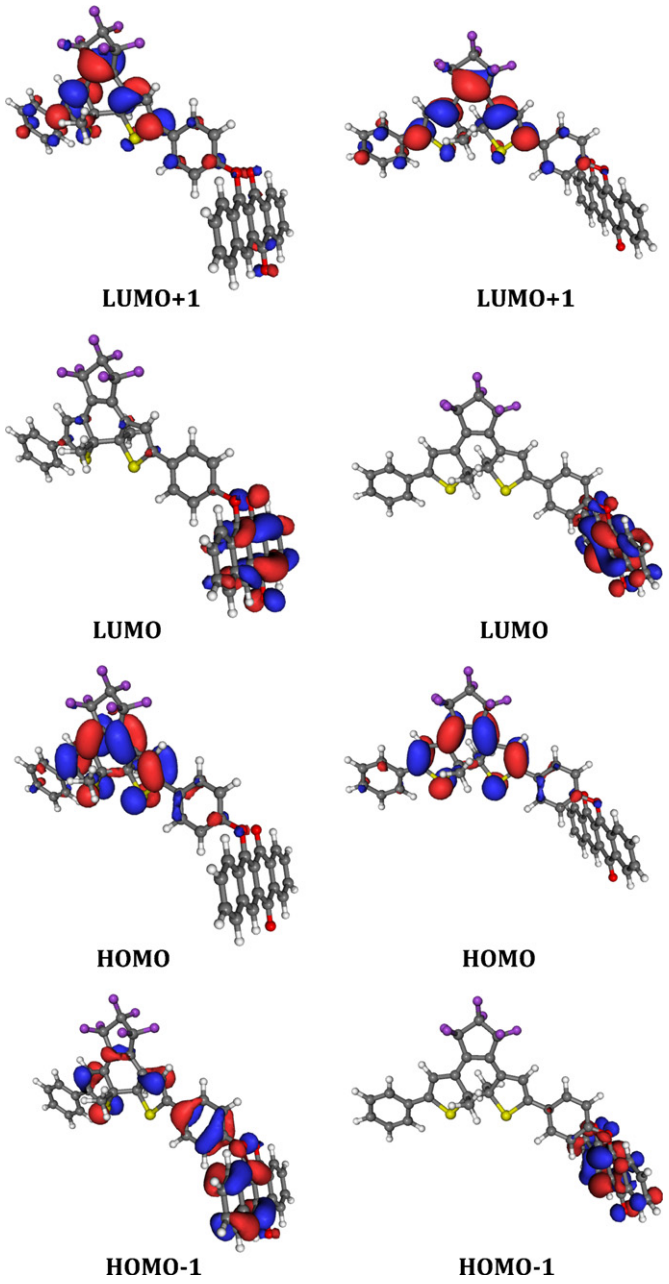

Fig. 6. Four frontier orbitals of **III-ct** (left) and **III-ca** (right). See caption of Fig. 4 for more details.

For **I-a**, the λ_{max} almost exclusively corresponds to an HOMO → LUMO electron promotion, whereas for **I-t**, smaller but non-negligible HOMO-1 → LUMO and HOMO-5 → LUMO contributions have additionally to be considered to interpret the first absorption band. The topology of these frontier orbitals is displayed in Fig. 4. Let us underline that, contrary to the DT case [39], these orbitals cannot qualitatively account for the actual photoisomer-

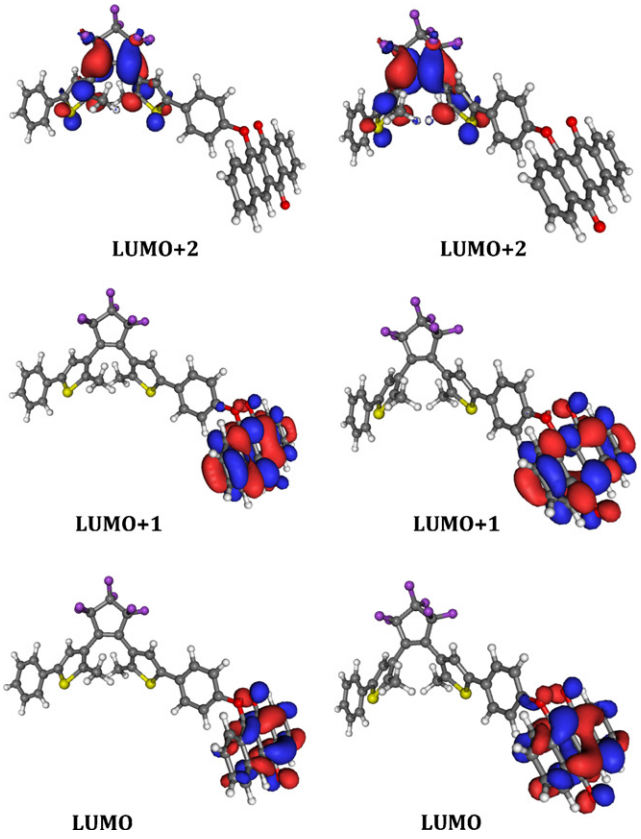

Fig. 7. First three virtual orbitals of **III-ot** (left) and **III-oa** (right). See caption of Fig. 6 for more details.

ization process as the involved mechanism is relatively complex for PNQ [54]. For the *ana* form, the phenyl ring plays a negligible role, both the HOMO and the LUMO being delocalized on the fused-ring center. On the contrary, for the **I-t**, the electronic excitation is associated to a partial electronic transfer from the phenyl ring to the central core. These findings hint that the substitution of hydrogen atoms of the phenyl ring with electroactive groups might affect more importantly the spectral features of the *trans* than the *ana* form. This prediction is validated by experimental evidences, as adding a *p*-NO_2 group on the phenyl ring induces an hypsochromic displacement of −5 nm for the *trans* isomer (CAM-B3LYP estimate: −6 nm [71]), but has no significant influence on the *ana* UV/vis spectrum [52]. To impact on this latter form, one should rely on bulkier substituents (e.g. 2,4,6-Me, see Ref. [52]) that probably alter the relative orientations of the two aromatic groups.

3.3. Multi-addressable structure

The absorption wavelengths computed for the four possible forms of Branda's DT/PNQ hybrid (Fig. 2) can be found in Table 2. Cartesian coordinates and complete TD-DFT results can be found as Supplementary Data. Both functionals provide relatively consistent results [72] with deviations in the line of Section 3.1. By comparing the data listed in Tables 1 and 2, it appears that the electronic spectra of the hybrid can be seen as the simple superposition of the bands of both photochromes, at least within the visible domain (see Fig. 5). This statement is in complete agreement with experimental measurements [17]. The same nearly additive pattern holds for the relative Gibbs free energies that are 0.0 kcal mol^{-1} (**III-ot**), 8.3 kcal mol^{-1} (**III-oa**), 9.8 kcal mol^{-1} (**III-ct**) and 19.1 kcal mol^{-1} (**III-ca**).

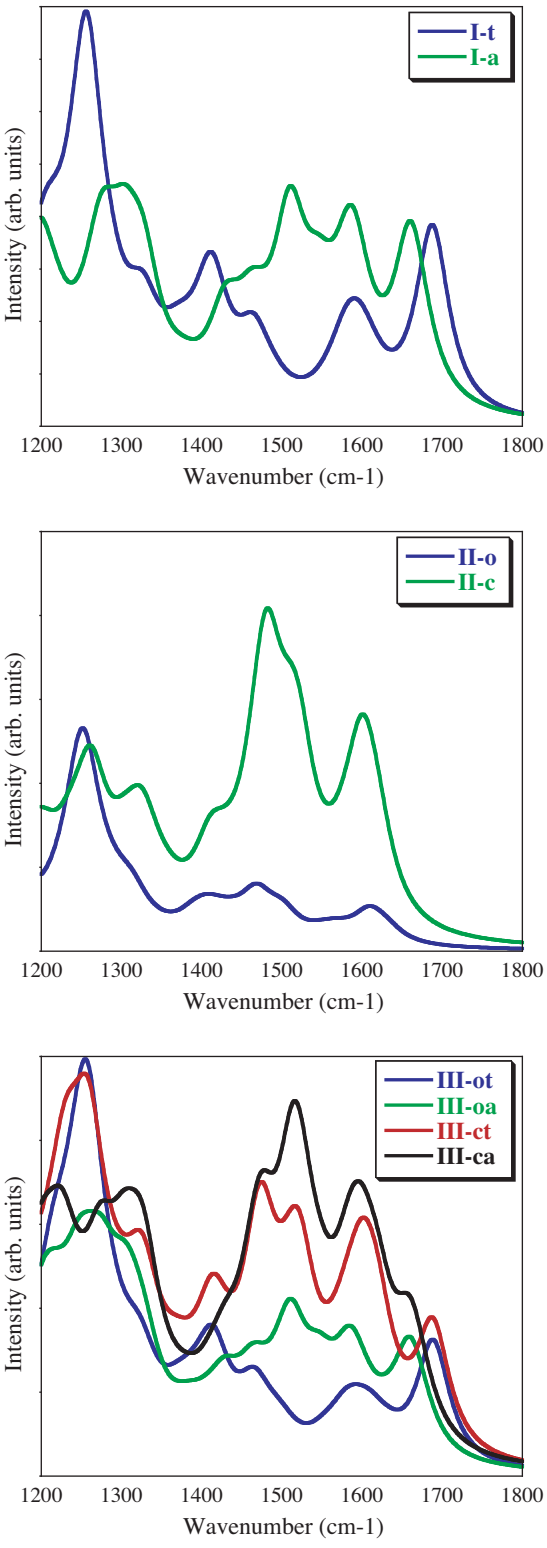

Fig. 8. Simulated PCM-PBE0/6-311G(d,p) IR spectra for **I**, **II** **III**. A broadening Lorentzian (FWHM = 50 cm^{-1}) and a scaling factor of 0.96 have been used. The same curves using a FWHM of 5 cm^{-1} are available as Supplementary Data.

When the DT is closed, the main contribution of the band close to 600 nm is mainly related to an HOMO → LUMO+1 transition (with a small HOMO → LUMO component) for both **III-ca** and **III-ct**. These orbitals, represented in Fig. 6, are completely localized on the DT moiety and present the expected shapes [39]. Indeed, the HOMO

Table 2
Theoretical λ_{max} (nm) for the four isomers of **III**. Only the main absorption bands are listed (see Fig. 5 and Supplementary Data). Raw data correspond to the state (number, wavelength and oscillator strength) obtained through TD-DFT, orbital composition gives the largest orbital contribution for that transition whereas convoluted gives the results after convolution with a Gaussian.

Isomer	PBE0			CAM-B3LYP		
	Raw data	Orbital composition	Convoluted	Raw data	Orbital composition	Convoluted
III-ot	S_5: 388 (0.19)	H-2 → L	387 (0.24)	S_2: 349 (0.16)	H-2 → L	345 (0.23)
III-oa	S_2: 479 (0.33)	H-2 → L	477 (0.37)	S_1: 454 (0.42)	H-2 → L	454 (0.42)
	[a]		360 (0.13)	[a]		400 (0.17)
				S_7: 311 (0.12)	H-1 → L+2	304 (0.19)
				S_8: 297 (0.11)	H-10 → L	
III-ct	S_1: 634 (0.56)	H → L+1	632 (0.56)	S_1: 573 (0.56)	H → L+1	574 (0.56)
	S_6: 389 (0.16)	H-2 → L		S_4: 344 (0.36)	H-1 → L	342 (0.58)
	S_8: 365 (0.22)	H → L+3		S_5: 343 (0.17)	H-1 → L+1	
	S_{10}: 357 (0.51)	H-1 → L+1	360 (0.76)	S_7: 321 (0.22)	H → L+3	
				S_{10}: 300 (0.66)	H-3 → L+1	301 (0.72)
III-ca	S_2: 630 (0.49)	H → L+1	629 (0.49)	S_1: 577 (0.56)	H → L+1	577 (0.56)
	S_3: 486 (0.36)	H-1 → L	484 (0.37)	S_2: 455 (0.37)	H-1 → L	451 (0.42)
				S_4: 426 (0.13)	H → L	
	[a]		384 (0.10)	S_6: 345 (0.31)	H-2 → L+1	338 (0.40)
				S_8: 321 (0.18)	H → L+3	

[a] Several small contributions, all having $f < 0.1$, see Supplementary Data.

is centered on the double bonds whereas the LUMO+1 presents a topology similar to the open-DT ground-state. It is therefore not surprising that irradiation with a wavelength larger than 557 nm, that promotes the electron to the LUMO+1, subsequently induces the ring-opening reaction of the DT without affecting the PNQ group [17]. The second band, close to 460 nm for **III-ca** and 350 nm for **III-ct** principally originates in an HOMO-1 → LUMO transition, but with several smaller contributions in both cases. As can be seen in Fig. 6, for **III-ca** these two orbitals are well localized on the PNQ side. For **III-ct**, this statement holds only for the LUMO, the HOMO-1 being delocalized on the full structure, and this follows the analysis performed in Section 3.2 for *trans* PNQ. This finding hints that though the experimental and theoretical spectra are a simple superposition of separated photochromes, the electronic communication between the two sides is not completely hindered. Nevertheless, this effect should have a negligible impact on the photochromic reactivity as the conjugation is only effective in the ground-state (occupied orbitals).

For **III-oa**, the three first virtual orbitals, that are the most significant for the photochromic activity [5,39], are represented in Fig. 7. It is obvious that one should promote the electron to the LUMO+2 to initiate the ring-closure of the DT: this orbital benefits from a significant density on both reactive carbon atoms and presents a bonding character for the to-be-formed CC bond [73]. On the contrary, both the LUMO+1 and the LUMO are centered on PNQ without contributions on the DT side. By inspecting all transitions computed at the TD-DFT level, it appears that the first transition implying the LUMO+2 is located at 311 nm (CAM-B3LYP) and this perfectly fits experimental evidences as the irradiation of **III-oa** with a 313 nm light allows the open to close conversion of the DT [17]. On the other hand, the band at 454 nm (Fig. 5) only includes the LUMO: TD-DFT predicts that irradiation above 434 nm should only influence the PNQ switch, and this is consistent with Ref. [17]. For **III-ot**, the two largest contributions to the absorption band at 345 nm (CAM-B3LYP) are HOMO-2 → LUMO and HOMO → LUMO. As can be seen in Fig. 7, the situation is similar to **III-ot**, with the LUMO and LUMO+1 (LUMO+2) related to the PNQ (DT) side. Considering the TD-CAM-B3LYP results, the orbital contributions are nicely separated for all peaks above 300 nm, the LUMO (LUMO+2) being dominant in the 348 nm (311 nm) transition presenting an oscillator strength of 0.16 (0.11). As can be seen in Table 2, these two peaks together with smaller contributions lead to an absorption at 345 nm after convolution.

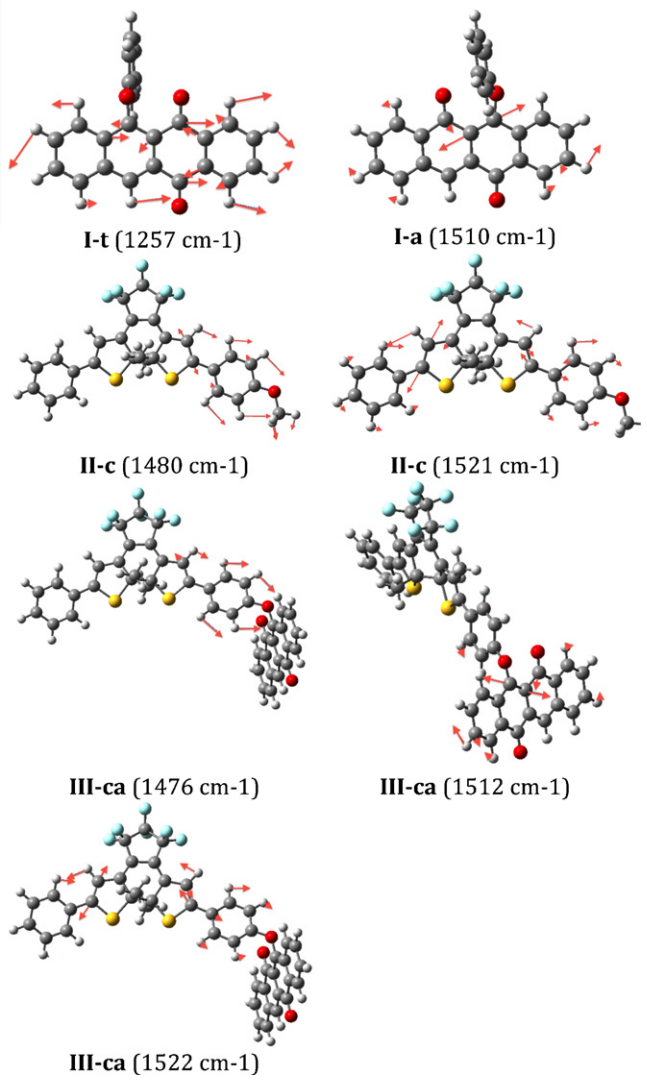

Fig. 9. Representation of the most important vibrational modes for selected structures. Note that the reported wavenumbers have been scaled (see caption of Fig. 8). See text for more details.

Eventually, we have simulated the infrared spectra of the four isomers and compared the results to similar calculations performed for the two model systems (see Fig. 8 and Supplementary Data). It turned out that the most sensitive vibrational region is close to 1500 cm^{-1}, so we will focus our analysis in the 1200–1800 cm^{-1} domain. For PNQ, going from the *trans* to the *ana* form induces a strong decrease of intensity around 1250 cm^{-1}. The principal mode corresponding to this band is presented in Fig. 9 and includes both hydrogen bendings and CC stretchings. When going to the *ana* form, one notes both a sharp decrease of this band, and the emergence of a contribution around 1500 cm^{-1}. This new band mainly involves the stretching of two carbon atoms (see Fig. 9). Obviously, for both PNQ forms, these two signatures do not involve significantly the phenyl ring. For the DA, the electro-cyclization implies a significant boost of the IR intensity around 1500 and 1600 cm^{-1}. The two modes that dominate in the strong 1500 cm^{-1} band of **II-c** are shown in Fig. 9 and imply both the DA core and the side *p*-OMe-Ph group. Let us now turn towards the DT/PNQ hybrid and start with the less conjugated form, **III-ot**. In that case, the spectra is almost unchanged with respect to **I-t** and the contribution of the DT side is quite negligible. Indeed, the most intense band (1260 cm^{-1}) is clearly PNQ-centered. When going to **III-oa**, the same conclusion holds: the major vibrational movements are located on the PNQ side. In other words, the contribution of DT only becomes obvious when it is closed. For **III-ct**, one conserves the 1250 cm^{-1} absorption typical of *trans*-PNQ and the peaks at 1500 and 1600 cm^{-1} indicating a close DT. Eventually, for the most conjugated **III-ca**, the vibrational modes of **I-a** and **II-c** are added to produce a very intense structured band. Many individual normal modes contribute. The three most intense can be found in Fig. 9 and clearly indicate a quasi independence of the two sides of the molecule.

4. Summary and outlook

Using a time-dependent density functional theory approach accounting for bulk solvent effects, we have simulated the properties of dithienylethene and phenoxynaphthacenequinone photochromes, separately and bonded together. It turns out that TD-DFT is able to reproduce accurately the position of the main absorption bands of both photochromes. For the DT side, CAM-B3LYP emerges as the most accurate with very small deviations; on the contrary, for the PNQ, PBE0 outperforms the range-separated hybrids. For Branda's DT/PNQ hybrid, an examination of the orbitals participating to each electronic transition provides a picture consistent with experimental measurements. In this twin photochrome structure, the electronic communication between the two entities is limited (though not completely impeded): the blend behaves like the superposition of two photochromes. This parallels silicon-linked DT dimers [11], for which a complete photochromic activity has also been observed. We are therefore currently working on a quantum mechanical strategy to optimize the properties of coupled photochromes, such that (i) full photochromism is preserved and (ii) all photochromes cooperate so to avoid that the final architecture remains a simple addition of two independent building blocks.

Acknowledgments

D.J. is indebted to the *Région des Pays de la Loire* for financial support in the framerwok of a *recrutement sur poste stratégique*. This research used resources of the Interuniversity Scientific Computing Facility located at the University of Namur, Belgium, which is supported by the F.R.S.-FNRS under convention No. 2.4617.07.

Appendix A. Supplementary data

Supplementary data associated with this article can be found, in the online version, at doi:10.1016/j.jphotochem.2010.11.021.

References

[1] H. Dürr, H. Bouas-Laurent, Photochromism: Molecules and Systems, Elsevier, New York, 2003.
[2] V. Balzani, A. Credi, M. Venturi, Molecular Devices and Machines — A Journey into Nano World, Wiley–VCH, Weinheim, 2004.
[3] J. Areephong, H. Logtenberg, W.R. Browne, B.L. Feringa, Symmetric six-fold arrays of photo- and electrochromic dithienylethene switches, Org. Lett. 12 (2010) 2132–2135.
[4] D. Jacquemin, E.A. Perpète, F. Maurel, A. Perrier, Ab initio investigation of the electronic properties of coupled dithienylethenes, J. Phys. Chem. Lett. 1 (2010) 434–438.
[5] D. Jacquemin, E.A. Perpète, F. Maurel, A. Perrier, Doubly closing or not? Theoretical analysis for coupled photochomes, J. Phys. Chem. C 114 (2010) 9489–9497.
[6] A. Peters, N.R. Branda, Linked photochromism in covalently linked double 1,2-dithienylethenes, Adv. Mater. Opt. Electron. 10 (2000) 245–249.
[7] T. Kaieda, S. Kobatake, H. Miyasaka, M. Murakami, N. Iwai, Y. Nagata, A. Itaya, M. Irie, Efficient photocyclization of dithienylethene dimer, trimer, and tetramer: quantum yield and reaction dynamics, J. Am. Chem. Soc. 124 (2002) 2015–2024.
[8] I. Jung, H. Choi, E. Kim, C.H. Lee, S.O. Kang, J. Ko, Synthesis and photochromic reactivity of macromolecules incorporating four dithienyleethene units, Tetrahedron 61 (2005) 12256–12263.
[9] H. Choi, I. Jung, K.H. Song, K. Song, D.S. Shin, S.O. Kang, J. Ko, Synthesis and photochromic reactivity of diarylethene trimers bridged by ethenyl and ethynyl unit, Tetrahedron 62 (2006) 9059–9065.
[10] S. Kobatake, M. Irie, Synthesis and photochromic reactivity of a diarylethene dimer linked by a phenyl group, Tetrahedron 59 (2003) 8359–8364.
[11] J. Areephong, W.R. Browne, B.L. Feringa, Three-state photochromic switching in a silyl bridged diarylethene dimer, Org. Biomol. Chem. 5 (2007) 1170–1174.
[12] T. Mrozek, H. Görner, J. Daub, Towards multifold cycloswitching of biphotochromes: investigation on a bond-fused dihydroazulene/vinylheptafulvene and dithienylethene/dihydrothienobenzothiophene, Chem. Commun. (1999) 1487–1488.
[13] T. Mrozek, H. Görner, J. Daub, Multimode-photochromism based on strongly coupled dihydroazulene and diarylethene, Chem. Eur. J. 7 (2001) 1028–1040.
[14] F. Ortica, D. Levi, P. Brun, R. Guglielmetti, G. Mazzucato, G. Favaro, Photokinetic behaviour of biphotochromic supramolecular systems part 2. a bis-benzochromene and a spirooxazinechromene with a (z-)ethenic bridge between each moiety, J. Photochem. Photobiol. A: Chem. 139 (2001) 133–141.
[15] G. Favaro, D. Levi, F. Ortica, A. Samat, R. Guglielmetti, U. Mazzucato, Photokinetic behaviour of bi-photochromic supramolecular systems part 3. compounds with chromene and spirooxazine units linked through ethane, ester and acetylene bridges, J. Photochem. Photobiol. A: Chem. 149 (2002) 91–100.
[16] A. Samat, V. Lokshin, K. Chamontin, D. Levi, G. Pepe, R. Guglielmetti, Synthesis and unexpected photochemical behaviour of biphotochromic systems involving spirooxazines and naphthopyrans linked by an ethylenic bridge, Tetrahedron 57 (2001) 7349–7359.
[17] A.J. Myles, T.J. Wigglesworth, N.R. Branda, A multi-addressable photochromic 1,2-dithienylcyclopentene–phenoxynaphthacenequinone hybrid, Adv. Mater. 15 (2003) 745–748.
[18] M. Frigoli, G.H. Mehl, Multiple addressing in a hybrid biphotochromic system, Angew. Chem. Int. Ed. Engl. 44 (2005) 5048–5052.
[19] S. Delbaere, G. Vermeersch, M. Frigoli, G.H. Mehl, Controlled conversion of isomers in a hybrid biphotochromic system, Org. Lett. 8 (2006) 4931–4934.
[20] S. Delbaere, J.C. Micheau, M. Frigoli, G.H. Mehl, G. Vermeersch, Mechanistic understanding of the photochromism of a hybrid dithienylethene– naphthopyran system by NMR spectroscopy, J. Phys. Org. Chem. 20 (2007) 929–935.
[21] S. Delbaere, G. Vermeersch, M. Frigoli, G.H. Mehl, Bridging the visible: the modulation of the absorption by more than 450 nm, Org. Lett. 12 (2010) 4090–4093.
[22] D. Jacquemin, E.A. Perpète, F. Maurel, A. Perrier, Hybrid dithienylethene–naphthopyran multi-addressable photochromes: an ab initio analysis, Phys. Chem. Chem. Phys. 12 (2010) 13144–13152.
[23] G. Sevez, J. Gan, S. Delbaere, G. Vermeersch, L. Sanguinet, E. Levillain, J.L. Pozzo, Photochromic performance of a dithienylethene–indolinooxazolidine hybrid, Photochem. Photobiol. Sci. 9 (2010) 131–135.
[24] E. Runge, E.K.U. Gross, Density-functional theory for time-dependent systems, Phys. Rev. Lett. 52 (1984) 997–1000.
[25] M.E. Casida, Time-Dependent Density-Functional Response Theory for Molecules, volume 1 of Recent Advances in Density Functional Methods, World Scientific, Singapore, 1995, pp. 155–192.
[26] D. Jacquemin, E.A. Perpète, I. Ciofini, C. Adamo, Accurate simulation of optical properties in dyes, Acc. Chem. Res. 42 (2009) 326–334.
[27] C. Adamo, V. Barone, Toward reliable density functional methods without adjustable parameters: the PBE0 model, J. Chem. Phys. 110 (1999) 6158–6170.
[28] M. Ernzerhof, G.E. Scuseria, Assessment of the Perdew–Burke–Ernzerhof exchange-correlation functional, J. Chem. Phys. 110 (1999) 5029–5036.
[29] D. Jacquemin, E.A. Perpète, Ab initio calculations of the colour of closed-ring diarylethenes: TD-DFT estimates for molecular switches, Chem. Phys. Lett. 429 (2006) 147–152.

[30] T. Yanai, D.P. Tew, N.C. Handy, A new hybrid exchange-correlation functional using the coulomb-attenuating method (CAM-B3LYP), Chem. Phys. Lett. 393 (2004) 51–56.
[31] J.D. Chai, M. Head-Gordon, Long-range corrected hybrid density functionals with damped atom–atom dispersion corrections, Phys. Chem. Chem. Phys. 10 (2008) 6615–6620.
[32] M.J.G. Peach, P. Benfield, T. Helgaker, D.J. Tozer, Excitation energies in density functional theory: an evaluation and a diagnostic test, J. Chem. Phys. 128 (2008) 044118.
[33] D. Jacquemin, V. Wathelet, E.A. Perpète, C. Adamo, Extensive TD-DFT benchmark: singlet-excited states of organic molecules, J. Chem. Theory Comput. 5 (2009) 2420–2435.
[34] L. Goerigk, S. Grimme, Assessment of TD-DFT methods and of various spin scaled cis(d) and cc2 versions for the treatment of low-lying valence excitations of large organic dyes, J. Chem. Phys. 132 (2010) 184103.
[35] D. Jacquemin, E.A. Perpète, I. Ciofini, C. Adamo, Assessment of the ωb97 family for excited-state calculations, Theor. Chem. Acc. in press, doi:10.1007/s00214-010-0783-x.
[36] M.J. Frisch, G.W. Trucks, H.B. Schlegel, G.E. Scuseria, M.A. Robb, J.R. Cheeseman, G. Scalmani, V. Barone, B. Mennucci, G.A. Petersson, H. Nakatsuji, M. Caricato, X. Li, H.P. Hratchian, A.F. Izmaylov, J. Bloino, G. Zheng, J.L. Sonnenberg, M. Hada, M. Ehara, K. Toyota, R. Fukuda, J. Hasegawa, M. Ishida, T. Nakajima, Y. Honda, O. Kitao, H. Nakai, T. Vreven, J.A. Montgomery Jr., J.E. Peralta, F. Ogliaro, M. Bearpark, J.J. Heyd, E. Brothers, K.N. Kudin, V.N. Staroverov, R. Kobayashi, J. Normand, K. Raghavachari, A. Rendell, J.C. Burant, S.S. Iyengar, J. Tomasi, M. Cossi, N. Rega, J.M. Millam, M. Klene, J.E. Knox, J.B. Cross, V. Bakken, C. Adamo, J. Jaramillo, R. Gomperts, R.E. Stratmann, O. Yazyev, A.J. Austin, R. Cammi, C. Pomelli, J.W. Ochterski, R.L. Martin, K. Morokuma, V.G. Zakrzewski, G.A. Voth, P. Salvador, J.J. Dannenberg, S. Dapprich, A.D. Daniels, O. Farkas, J.B. Foresman, J.V. Ortiz, J. Cioslowski, D.J. Fox, Gaussian 09 Revision A.02, Gaussian Inc., Wallingford, CT, 2009.
[37] J. Tomasi, B. Mennucci, R. Cammi, Quantum mechanical continuum solvation models, Chem. Rev. 105 (2005) 2999–3094.
[38] D.Z. Chen, Z. Wang, X. Zhao, Z. Hao, Theoretical study on geometric electronic structures and absorption wavelengths properties of closed-ring isomers of diarylmaleic anhydrides, J. Mol. Struct. (Theochem.) 774 (2006) 77–81.
[39] A. Perrier, F. Maurel, J. Aubard, Theoretical investigation of the substituent effect on the electronic and optical properties of photochromic dithienylethene derivatives, J. Photochem. Photobiol. A: Chem. 189 (2007) 167–176.
[40] A. Perrier, F. Maurel, J. Aubard, Theoretical study of the electronic and optical properties of photochromic dithienylethene derivatives connected to small gold clusters, J. Phys. Chem. A 111 (2007) 9688–9698.
[41] A. Staykov, D. Nozaki, K. Yoshizawa, Photoswitching of conductivity through a diarylperfluorocyclopentene nanowire, J. Phys. Chem. C 111 (2007) 3517–3521.
[42] G. Callierotti, A. Bianco, C. Castiglioni, C. Bertarelli, G. Zerbi, Modulation of the refractive index by photoisomerization of diarylethenes: theoretical modeling, J. Phys. Chem. A 112 (2008) 7473–7480.
[43] F. Maurel, A. Perrier, E.A. Perpète, D. Jacquemin, A theoretical study of the perfluoro-diarylethenes electronic spectra, J. Photochem. Photobiol. A: Chem. 199 (2008) 211–223.
[44] P.D. Patel, A.E. Masunov, Theoretical study of photochromic compounds. 1. Bond length alternation and absorption spectra for the open and closed forms of 29 diarylethene derivatives, J. Phys. Chem. A 113 (2009) 8409–8414.
[45] V. Aubert, E. Ishow, F. Ibersiene, A. Boucekkine, J.A.G. Williams, L. Toupet, R. Metivier, K. Nakatani, V. Guerchais, H. Le Bozec, A reverse interrupter: the novel molecular design of a fluorescent photochromic DTE-based bipyridine, New J. Chem. 33 (2009) 1320–1323.
[46] P.D. Patel, I.A. Mikhailov, K.D. Belfield, A.E. Masunov, Theoretical study of photochromic compounds. 2. Thermal mechanism for byproduct formation and fatigue resistance of diarylethenes used as data storage materials, Int. J. Quantum Chem. 109 (2009) 3711–3722.
[47] A. Staykov, K. Yoshizawa, Photochemical reversibility of ring-closing and ring-opening reactions in diarylperfluorocyclopentenes, J. Phys. Chem. C 113 (2009) 3826–3834.
[48] D. Jacquemin, C. Michaux, E.A. Perpète, F. Maurel, A. Perrier, Photochromic molecular wires: insights from theory, Chem. Phys. Lett. 488 (2010) 193–197.
[49] N. Adami, D. Fazzi, A. Bianco, C. Bertarelli, C. Castiglioni, Enhancing the light driven modulation of the refractive index in organic photochromic materials: a quantum chemical strategy, J. Photochem. Photobiol. A: Chem. 214 (2010) 61–68.
[50] D. Jacquemin, E.A. Perpète, F. Maurel, A. Perrier, TD-DFT simulations of the electronic properties of star-shaped photochromes, Phys. Chem. Chem. Phys. 12 (2010) 7994–8000.
[51] D. Jacquemin, E.A. Perpète, G.E. Scuseria, I. Ciofini, C. Adamo, TD-DFT performance for the visible absorption spectra of organic dyes: conventional versus long-range hybrids, J. Chem. Theory Comput. 4 (2008) 123–135.
[52] Y.E. Gerasimenko, A.A. Parshutkin, N.T. Poteleshchenko, V.P. Poteleshchenko, V.V. Romanov, Photochromism of peri-aryloxy-p-quinones. Determination of molar extinction coefficients of 6-phenoxy-5,11-naphthacenequinones, Zhur. Prik. Spektro 30 (1979) 954–956.
[53] Z. Fang, S.Z. Wang, Z.F. Yang, B. Chen, F.T. Li, J.Q. Wang, S.X. Xu, Z.J. Jiang, T.R. Fang, Synthesis and photochromism in solution of phenoxynaphthacenequinone derivatives, J. Photochem. Photobiol. A: Chem. 88 (2005) 23–30.
[54] R. Born, W. Fischer, D. Heger, B. Tokarczyk, J. Wirz, Photochromism of phenoxynaphthacenequinones: diabatic or adiabatic phenyl group transfer? Photochem. Photobiol. Sci. 6 (2007) 552–559.
[55] D. Jacquemin, J. Preat, M. Charlot, V. Wathelet, J.M. André, E.A. Perpète, Theoretical investigation of substituted anthraquinone dyes, J. Chem. Phys. 121 (2004) 1736–1743.
[56] D. Jacquemin, X. Assfeld, J. Preat, E.A. Perpète, Comparison of theoretical approaches for predicting the UV/vis spectra of anthraquinones, Mol. Phys. 105 (2007) 325–331.
[57] The MAD of PBE0 is 18 nm/0.10 eV for the four states of Table 1, and this value can be compared to 23 nm/0.18 eV and 28 nm/0.22 eV differences for CAM-B3LYP and ωB97XD, respectively.
[58] D. Jacquemin, C. Peltier, I. Ciofini, Visible spectrum of naphthazarin investigated through time-dependent density functional theory, Chem. Phys. Lett. 493 (2010) 67–71.
[59] I.V. Rostov, R.D. Amos, R. Kobayashi, G. Scalmani, M.J. Frisch, Studies of the ground and excited-state surfaces of the retinal chromophore using CAM-B3LYP, J. Phys. Chem. B 114 (2010) 5547–5555.
[60] D. Jacquemin, C. Peltier, I. Ciofini, On the absorption spectra of recently synthesized carbonyl dyes: TD-DFT insights, J. Phys. Chem. A 114 (2010) 9579–9582.
[61] L. Jensen, N. Govind, Excited states of dna base pairs using long-range corrected time-dependent density functional theory, J. Phys. Chem. A 113 (2009) 9761–9765.
[62] B. Mennucci, C. Cappelli, C.A. Guido, R. Cammi, J. Tomasi, Structures and properties of electronically excited chromophores in solution from the polarizable continuum model coupled to the time-dependent density functional theory, J. Phys. Chem. A 113 (2009) 3009–3020.
[63] L. Zhang, X. Chen, H. Liu, L. Han, R.I. Cukier, Y. Bu, Exploration of the biological micro-surrounding effect on the excited states of the size-expanded fluorescent base x-cytosine in dna, J. Phys. Chem. B 114 (2010) 3726–3734.
[64] P. Zhao, D.S. Liu, S.J. Xiz, Ab initio investigation of the *i–v* characteristics of the phenoxynaphthacenequinone-based optical molecular switch, Phys. Lett. A 372 (2008) 5811–5815.
[65] P. Zhao, C.F. Fang, Y.M. Wang, Y.X. Zhai, D.S. Liu, First-principles study of the switching characteristics of the phenoxynaphthacenequinone-based optical molecular switch with carbon nanotube electrodes, Phys. E 41 (2009) 474–478.
[66] D. Jacquemin, E.A. Perpète, F. Maurel, A. Perrier, Simulation of the properties of a photochromic triad, J. Phys. Chem. Lett. 1 (2010) 2104–2108.
[67] T. Horii, Y. Abe, R. Nakao, Theoretical quantum chemical study of spironaphthoxazines and their merocyanines: thermal ring-opening reaction and geometric isomerization, J. Photochem. Photobiol. A: Chem. 119–129 (2001) 144.
[68] F. Maurel, J. Aubard, M. Rajzmann, R. Guglielmetti, A. Samat, A quantum chemical study of the ground state ring opening/closing of photochromic 1,3,3 trimethylspiro [indoline-2,3 naphtho-[1,4]oxazine], J. Chem. Soc., Perkin Trans. 2 (2002) 1307–1315.
[69] A. Perrier, F. Maurel, E.A. Perpète, V. Wathelet, D. Jacquemin, Spectral properties of spirooxazine photochromes: TD-DFT insights, J. Phys. Chem. A 113 (2009) 13004–13012.
[70] D. Jacquemin, A. Femenias, H. Chermette, J.M. André, E.A. Perpète, Second-order Möller-Plesset evaluation of the bond length alternation of several series of linear oligomers, J. Phys. Chem. A 109 (2005) 5734–5741.
[71] Using toluene as solvent for both the reference molecule and its nitro derivatives, so to be consistent with Ref. [52].
[72] However, PBE0 also predicts a weaker absorption band ($f \simeq 0.09$) at 574 nm for **III-oa**, and this band, not appearing in the experimental spectrum is probably a spurious-like state. The molecular orbital analysis is therefore performed with CAM-B3LYP that is more robust, even though it does not systematically allow minimal deviations with respect to experimental references.
[73] A.D. Laurent, J.M. André, E.A. Perpète, D. Jacquemin, Photochromic properties of dithienylazoles and other conjugated diarylethenes, J. Photochem. Photobiol. A: Chem. 192 (2007) 211–219.